

New Folder Name Intensity Noise

Charles C. Harb & Dr. Hans-A. Bachor

*Department of Physics and Theoretical Physics,
The Faculty of Science
Australian National University*

in collaboration with

**Peter Rottengatter, Dr. Ingo Kröpcke
& Prof. Herbert Welling**

*Laser Zentrum Hannover
Hollerithallee 8 D-W-3000 Hannover 21
Germany*

Reduction of the Intensity Noise in a Diode-Pumped Neodymium:YAG Nonplanar Ring Laser.

DITAC Report 1992

SUMMARY

This project was conducted at the laboratories of Laser Zentrum Hannover (LZH), in Hannover Germany, between 20th June and 1st November 1992. The aim of the project was to reduce the relative intensity noise (RIN) observed at the output of a diode pumped Nd:YAG nonplanar ring oscillator, caused by the phenomenon called relaxation oscillation. In this project we have shown that the regions of high RIN can be reduced by 40 to 50 dB using simple techniques that control the current driving the pump laser source, that is, the diode laser. Furthermore, we have shown that it is possible to produce a laser with quantum noise limited output at frequencies below 20kHz. In this report we will discuss the characteristics of the relaxation oscillation and then the specifics of the control loops developed to reduce this intensity noise.

Aim of this Collaboration

The group at the ANU has been developing several types of quantum noise limited sensors, such as polarimeters and interferometers, for use in the detection of weak electric and magnetic fields or very small ($<10^{-14}$ m) displacements. Such sensors require lasers which are shot noise limited in both intensity and frequency. The CW lasers, produced from a single crystal (monolithic) Neodymium:YAG laser pumped by semiconductor diode laser, that have been built at LZH are the best option for this research.

The aim of this project was to develop the technology that would stabilize the intensity and frequency of these laser systems. This report will outline the progress made in reducing the relative intensity noise (RIN) caused by the phenomenon called relaxation oscillation. This is an oscillation that occurs due to the tight coupling of energy between the cavity and population inversion of the laser. Relaxation oscillation leads to regions of high RIN in most solid state lasers.

Investigations into the control of frequency noise from these lasers is still in progress at LZH. The group at the ANU will continue the collaboration by assisting in the design and improvement of the laser system.

Scientific Progress

The Laser System

The laser system that we were working on is a diode pumped Nd:YAG non-planar ring oscillator. The lasing geometry is shown in figure 1. This design is based on the original design proposed by Kane *et al.*^{2,3}

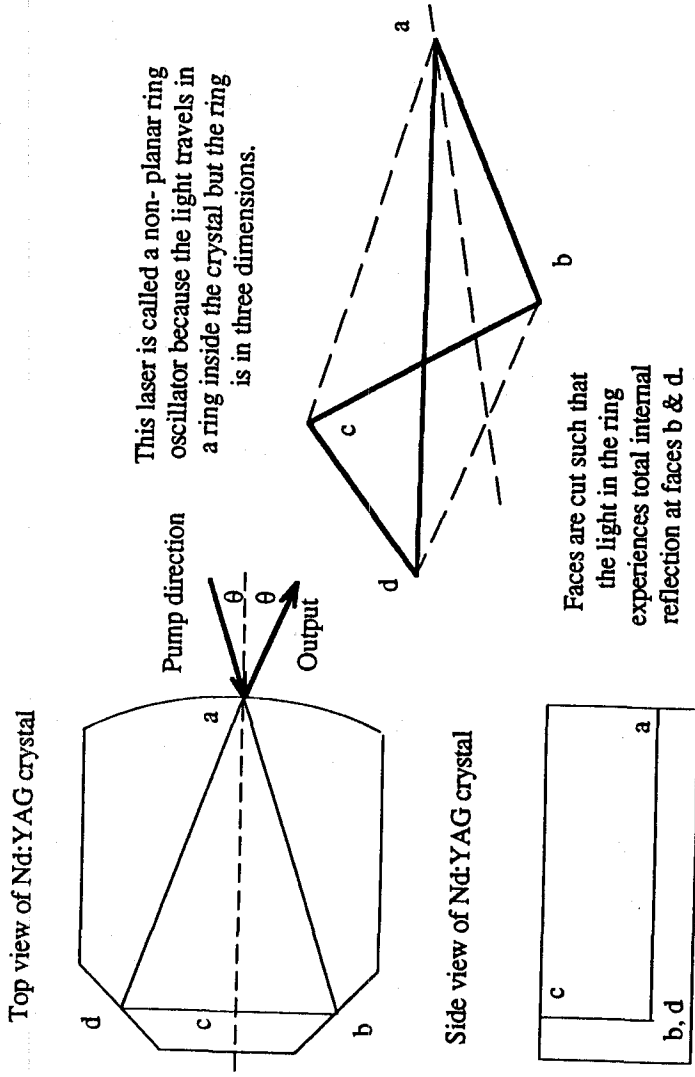


Figure 1. Schematic diagram showing the optical path inside the Nd:YAG ring oscillator. The pump laser follows the ray ab. The laser ring follows the path abcd. It folds out of the plane defined by abd at b, then folds back into that plane at c.

The pump source is a high power diode laser (1W typically) that is oscillating at 808.6nm. This pump source is chosen because the Nd:YAG has a high absorption efficiency at this wavelength, and also these high power diode lasers are commercially available. The output wavelength of these diode lasers is dependent on their operating temperature. The temperature is actively controlled to $\approx 300\text{K}$, however, it is set to the value which yields maximum absorption by the Nd:YAG. The laser diodes used in this project had an electrical power requirement of 1.4A at 2.5V to produce 1W optical power.

The light from the diode laser is focused into the Nd:YAG crystal by a short focal length lens ($\approx 50\text{ mm}$). Lasing occurs in the ring geometry shown in figure 1. The geometry of the

monolithic resonator is described by Nilsson⁴. The internal path of the resonator consists of two isosceles triangles with a common base line. These triangles are not in the same plane, they are forced to fold out of the plane as shown. This ring is thus known as a non-planar configuration. The ring geometry is chosen primarily to eliminate spatial hole burning inside the laser medium. Single frequency and unidirectional operation is achieved by placing a permanent magnet below the laser crystal. The magnetic field induces a polarisation rotation (Faraday effect) which, in turn, increases losses in one of the lasing directions and hence stops the lasing action. The nonplanar beam geometry is essential for this process to be operable. Some alterations* have been made in subsequent designs which we will not be elaborated on here because they were not implemented at the time of this work.

The passive output characteristics of the Nd:YAG laser are promising in their own right, compared to other passively stabilized laser systems such as dye lasers or gas lasers. The frequency noise arises from temperature fluctuations in the crystal, and produces 3 GHz/K³

* For example, LZH is no longer using a focusing lens for the diode laser and also the front face of the Nd:YAG is no longer curved. For further details contact the group at LZH.

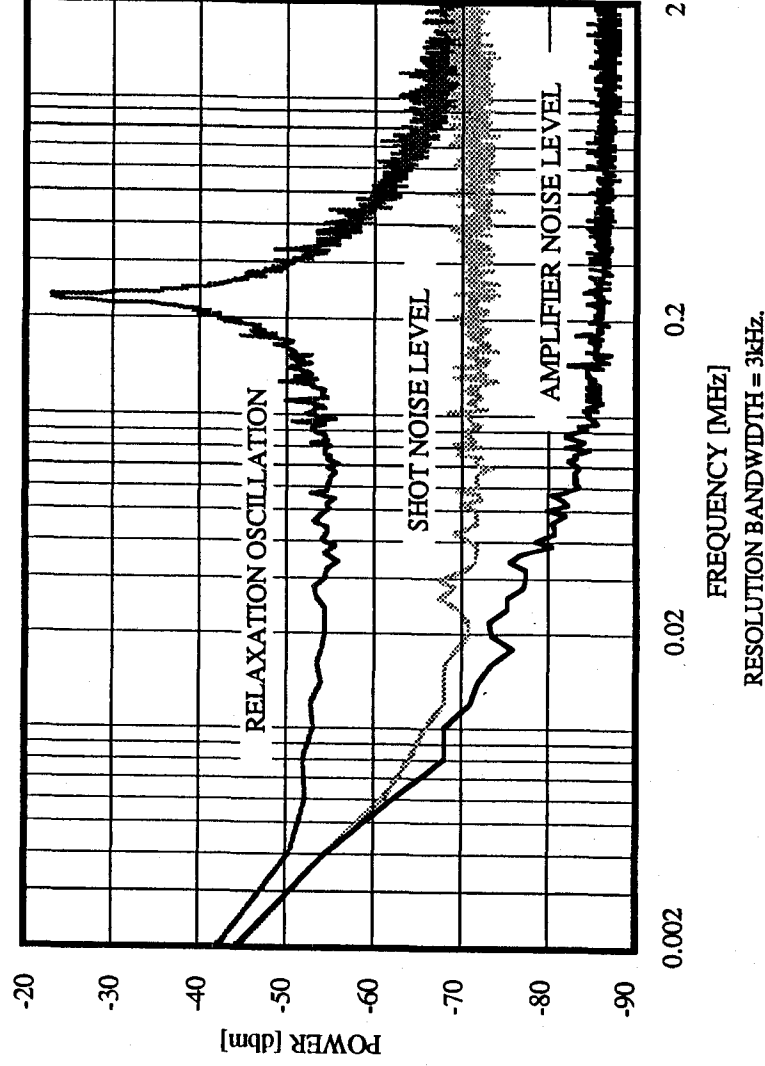


Figure 2. RF spectrum analyser scan showing : the noise from the relaxation oscillation that is inherent in the diode pumped Nd:YAG laser; the shot noise level produced by an equivalent amount of white light shining on the same photo-detector; the dark noise level of the photo-detector system. The relaxation oscillation generates noise above the shot noise limit from near DC to approximately 2MHz for this detection light level.

frequency change. With suitable temperature control^{6,7} the frequency fluctuations can be reduced to the MHz or even kHz level. Furthermore, it has been shown⁸ that standard RF locking techniques can reduce the frequency fluctuations to the hundreds of mHz level, and further improvements are being investigated continuously.

The intensity fluctuations of this system are also impressive compared to other systems. RIN is generally confined to frequencies below 10MHz². The particular laser that we were working with at LZH reached the shot noise level at ≈ 2 MHz with 4-5mW of laser light on the photodetector, see figure 2. Figure 2 shows the relaxation oscillation, the shot noise level for an equivalent photo-current passing through the detector, and the "dark" noise or amplifier noise level. It is important to ensure that there is sufficient separation between these three levels, otherwise suppression of the RIN to the shot noise level would not be possible¹⁰ due to excessive technical or classical noise. In other words, a large relaxation oscillation signal to amplifier noise ratio is required in the feedback loop.

The Control Electronics & Experimental Results

The detector circuit used to measure the noise traces of figure 2 is shown in figure 3. The circuit utilises a reverse biased silicon photo-detector, that has its signal amplified using a transimpedance configuration. In this case we chose the LM 6361 op-amp as the transimpedance amplifier because of its low noise and fast response (there is <10 degrees of input-output phase lag at 1MHz) properties. However, these amplifiers are not able to drive 50 Ω loads, hence the HA 5002 buffer amp was placed directly after the op-amp and ensured that there was no signal

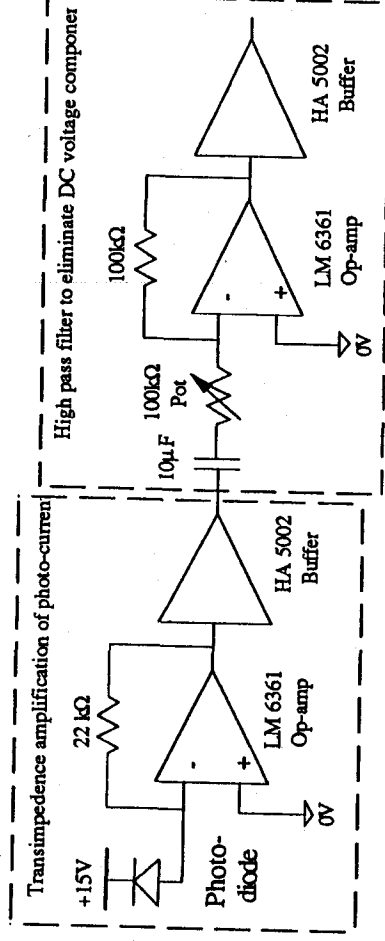


Figure 3. Schematic diagram of the photo-detector circuit used for this work. The actual photo-detector was a garden variety silicon detector (low quantum efficiency for the the output wavelength of this laser, but quite sufficient for this investigation). The photo-current is amplified by a fast op-amp. (National LM 6361) operating as a transimpedance amplifier, and then buffered (Harris HA 5002) for isolation. An active high pass filter (roll off at about 10 Hz) is placed after the transimpedance amplifier, and acts like a DC block.

degradation by other elements in the circuit. A 1.6Hz high pass filter was placed after the photo-detector circuit to eliminate the DC component. This photo-detection circuit was used in all the experiments described in this report.

Stabilization of intensity fluctuations for lasers has usually been achieved by using an electro-optic modulator (EOM), or acousto-optic modulator (AOM)¹¹. These modulators are generally external to the laser system. They regulate the intensity to some level less than the original output intensity level of the laser. Hence a loss of useful laser radiation is inherent to these techniques of intensity stabilization. One advantage of the diode-pumped Nd:YAG lasers is that the output intensity can be controlled by direct injection of a control signal into the current of the diode laser^{12,13,14} (this technique is shown schematically in figure 4). Only the AC components are effected by the control loop. Hence, little, if any, DC intensity is lost with this method.

Even though this technique is not new, prior to the collaboration all attempts at LZH to inject the error signal into the current of the diode laser had been limited to low frequency (<100kHz) due to inadequate injection of the signal. During this work we improved the technique for error signal injection (see figure 5) by sending the signal directly to the anode of the diode laser, hence by-passing the internal filters of the diode laser power supply. The connection was made as close as possible to the laser diode to ensure minimal transit delays.

There are two options shown in figure 5 for injection of the error signal, which shall be called the drive circuits. The first (fig. 5a) circuit was the one used for all the result produced in this report. In this method the final op-amp is held at the same voltage potential as the laser diode

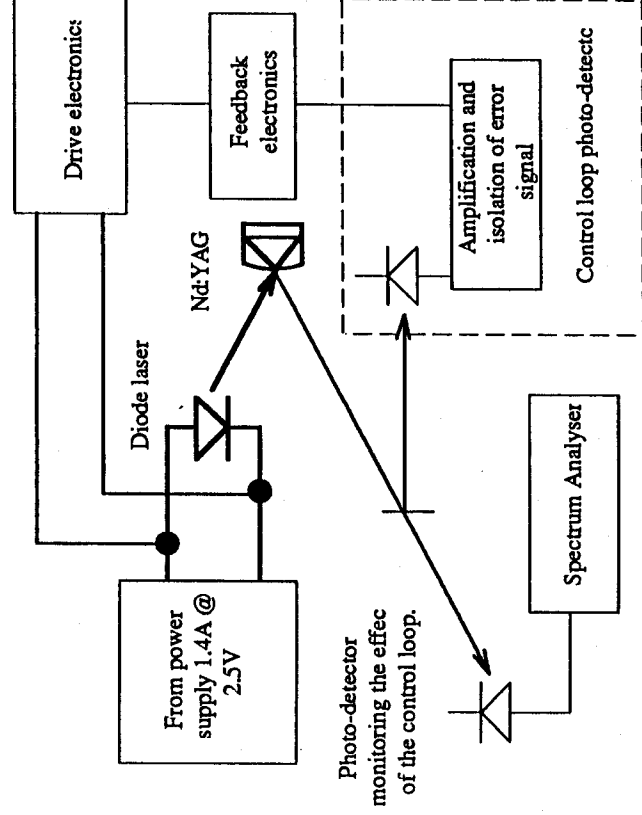


Figure 4. Block diagram of the control loop employed to reduce the relaxation oscillation. A fraction of the output from the Nd:YAG is sent to the control loop photo-detector where it is amplified then sent to the feedback electronics and the drive circuit electronics. The effects of the control loop on the output of the laser is independently detected using an external photo-detector.

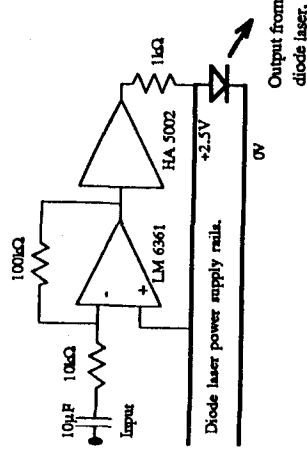


Figure 5a. The drive circuit electronics used in all the results presented in this report. The signal from the feedback electronics is AC coupled and amplified by a factor of 10 in this circuit. The amplifier is held at the same potential as the diode laser by adding its voltage to the positive input of the op-amp. The voltage from the buffer is converted to a current using a 1kΩ resistor.

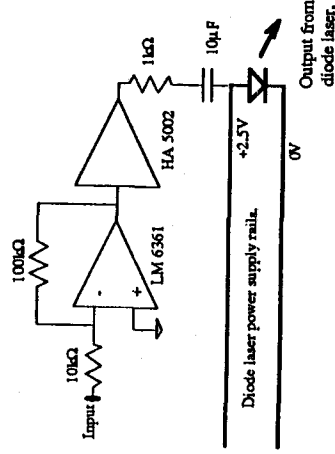


Figure 5b. An equivalent drive circuit to that of 5a which will be tested at a later stage. The advantage of this circuit is that the potential from the diode laser does not have to be added to the positive input of the op-amp.

by sampling the DC voltage at the diode laser and inserting this to the positive input of the op-amp. The error signal current was then coupled directly into the current of the laser using a 1kΩ resistor. It was latter shown that the AC coupling of the error signal produced the same outcome. Thus, the second method (fig. 5b) is an equivalent scheme to the first and will be tested at a later stage. In this method the drive circuit is AC coupled using a large capacitor (20μF for example), which will have minimal effect on the control loop.

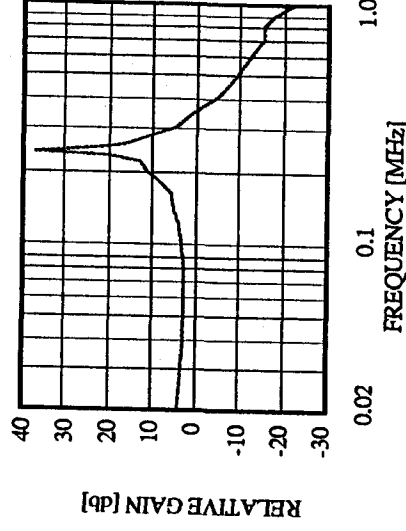
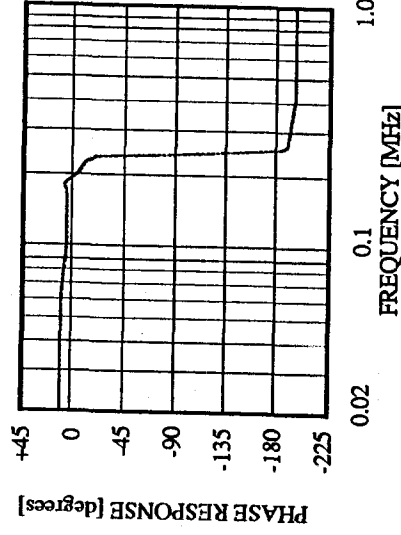


Figure 6. The phase and amplitude response across the relaxation oscillation. The phase at low frequencies starts slightly advanced with respect to the input signal, remains nearly constant until the relaxation oscillation frequency is reached where it changes phase by 180 degrees, then returns to being almost constant. In total 205 degree phase change is experienced from near DC to 1MHz. The amplitude is flat from near DC to the relaxation oscillation frequency then has high gain at the relaxation oscillation and rolls off at high frequencies.

The initial investigations were to determine the properties of the relaxation oscillation. These are shown in figure 6. The tests were performed by injecting a sinusoidally varying voltage at the input of the drive circuit and observing the effect on the output of the laser. Of particular interest was the gain and the phase response of the system across the relaxation oscillation. It was important to determine that the oscillation could be treated like a simple mechanical resonance. The results showed that this was indeed possible because the gain is constant at frequencies below the relaxation oscillation, then rises to a maximum at the

relaxation oscillation frequency, and then has a $1/f^2$ roll-off for frequencies above the relaxation frequency. Simultaneously, the phase response is almost constant at frequencies below the relaxation oscillation, changes by 180° across the relaxation oscillation, then is almost constant again for frequencies above the relaxation frequency.

The position of the relaxation oscillation is dependent on many factors such as the resonator and material properties, but for a given laser system the determining factor is the cavity photon density and therefore the optical output power. We were operating in the regime where the oscillation occurred at approximately 240kHz. In general, however, the output power can be varied by altering the pump power, hence the frequency of the relaxation oscillation is also variable. In this case, a control loop that can operate independent of the relaxation oscillation frequency is most desirable. Unfortunately, this may not be possible (as will be shown later in this report) and the control loop will need to be altered for different output powers of the laser system. The commercially available Nd:YAG lasers from Lightwave Electronics Corporation are operating with this restriction.

An ideal feedback control loop monitors the noise on the output of a free running system (such as that shown in figure 4) producing an error signal. It then sends a correction signal back to the system that is 180 degrees out of phase with the error signal, and has a magnitude at least as large as the noise. Technically, however, it is not possible to produce this type of signal for all frequencies in the noise spectrum because of the phase shifts in the amplifiers of the controller, the delays in feeding the signals back to the system and the phase shift associated with relaxation oscillation itself. We can compensate for the first two difficulties by using high speed operational amplifiers placed in close proximity to the system, but the third problem can not be overcome, rather we must force the error signal to change frequency properties using different types of active filters. The general type of filter used in controlling the phase and gain of the feedback signal is called a PID, which stands for *proportional-integrating-differentiating* amplifier. Before producing this full controller, we chose to use its separate sections to investigate the response of the system to them independently.

Results from three types of control loops will be presented here. Control loop 1 has a feedback section that supplies a frequency independent *proportional* amplification of the error signal to the drive circuit, for frequencies less than 1MHz. Control loop 2 has an active *differentiator* in its feedback section, and hence, supplies a signal that is advanced by 90 degrees and its gain is increasing at a rate of +6dB/octave with respect to the error signal. Finally, control loop 3 has an active *integrating* feedback loop. That is, the signal is lagging by 90 degree with respect to the error signal, and the gain is reducing at a rate of -6dB/octave. These control loops were placed in the position called feedback electronics of figure 4. The drive electronics and control loop photo-detector electronics remained unchanged throughout all the tests performed.

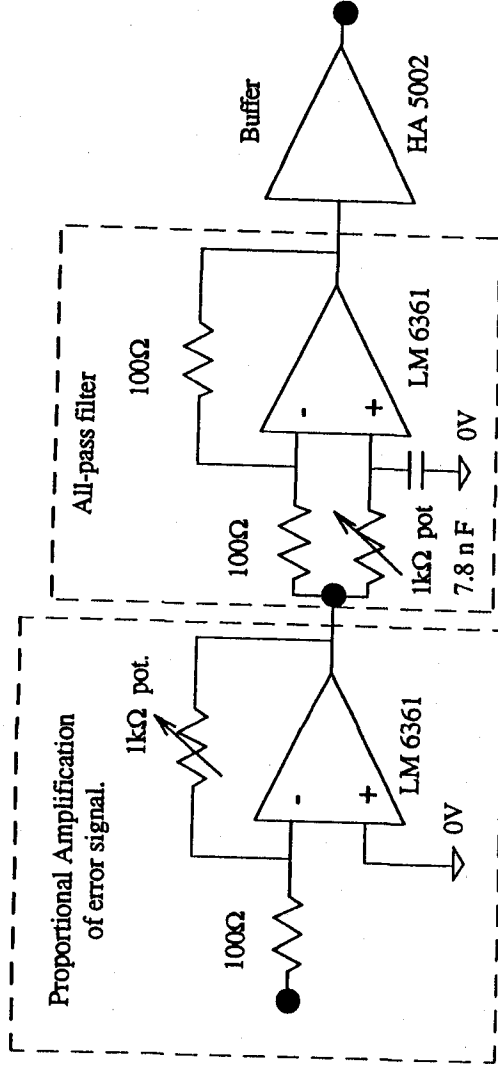


Figure 7a. Circuit diagram for control loop 1. This is an active proportional amplification of the error signal, maximum amplification factor is 10. It is followed by an all-pass filter which acts like a frequency delay element. The amount of delay is dependent on the resistance of the 1k Ω pot. Also, there is a buffer in the circuit for isolation.

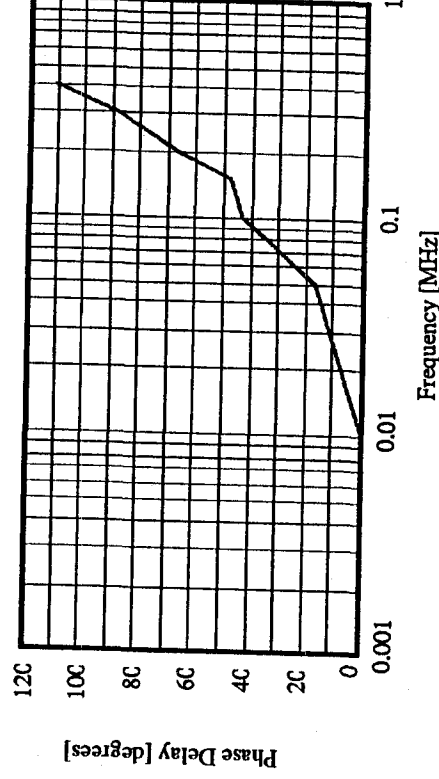
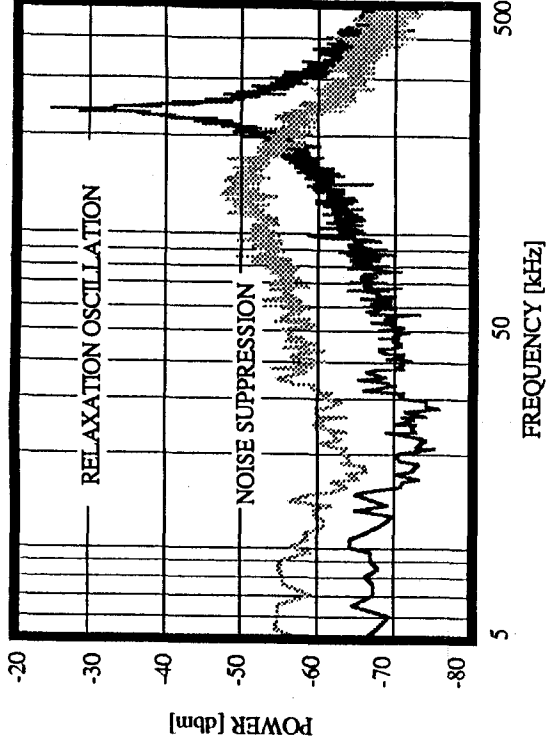


Figure 7b. The delay imposed by the all-pass filter for the results presented in fig. 8b.

The circuit diagram for control loop 1 is shown schematically in figure 7a. This circuit consists of a section that amplifies the error signal uniformly over the entire frequency range, followed by a section capable of altering the phase of the feedback signal, which is called an *all pass filter*. We used the all pass filter as a frequency dependent delay element in the control loop, as shown in figure 7b. All pass filters are not generally used in control loops because they impose transit delays of the error signal, which have to be compensated for at some stage in the loop. In this case, however, we were attempting to use this property to adjust the error signal arrival time (phase) at the point where it was being fed into the current of the diode laser.

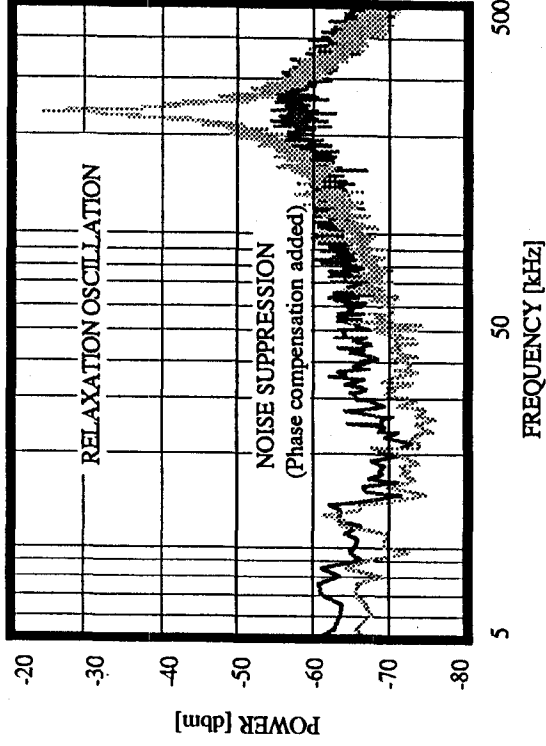
Using only the proportional section, the results of figure 8a were produced. The best noise suppression at the relaxation oscillation frequency was $\approx 34\text{dB}$, and also the noise at frequencies above the relaxation oscillation were significantly reduced ($\approx 5\text{dB}$ at 300kHz). However, the noise increased at frequencies below the relaxation oscillation by at least 15dB at 130kHz,

Figure 8a. Noise suppression achieved using only the proportional section of controller 1. The maximum suppression at the rel. osc. frequency is 34dB, however the noise is increased at frequencies below the rel. osc. Thus, the best suppression is only 23dB with this type of controller.



RESOLUTION BANDWIDTH = 3kHz.

Figure 8b. Noise suppression achieved using both the proportional and all-pass filter sections of controller 1. The phase compensation enabled an extra 15dB of noise reduction. However, a slight increase in low and high frequency noise was still present.



which was due to positive feedback at these frequencies. Hence only 23dB suppression overall was possible with this controller. Introducing some frequency dependent phase delay using the all pass filter resulted in better suppression at the relaxation oscillation frequency (\approx 38dB as shown in fig. 8b), but also less enhancement of the low frequency noise. A side effect of using the all pass filter was that the noise at frequencies above the relaxation oscillation frequency increased. Overall, the all pass filter improved the control loop properties and the best possible noise suppression was \approx 30dB. We concluded that a simple proportional controller could not solely be used to in the feedback electronics. This is unfortunate because this type of controller is independent of the frequency of the relaxation oscillation.

The circuit diagram for control loop 2 is shown in figure 9a. It consists of a section that has the properties of an active differentiator followed by an all pass filter, for phase adjustment of the feedback signal. The roll over frequency for the differentiator was chosen to be just lower

than the relaxation oscillation frequency, about 200kHz, so that the low frequency components in the error signal could be suppressed. Subsequently we could increase the gain of the higher frequency components in the error signal without increasing the low frequency noise of the laser, as was done in control loop 1.

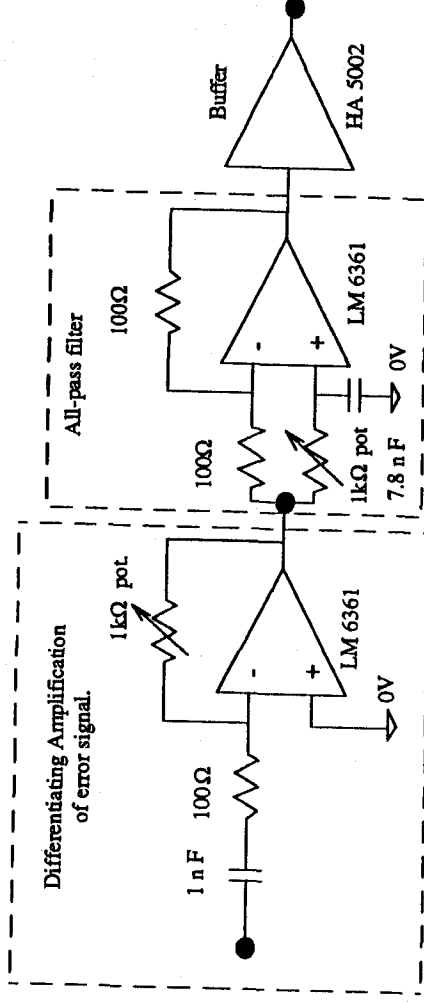


Figure 9a. Circuit diagram for control loop 2. This loop consist of an active high pass filter (roll off at 200kHz) followed by an all-pass filter and buffer. Once again the all-pass filter was used to adjust the phase of the control signal.

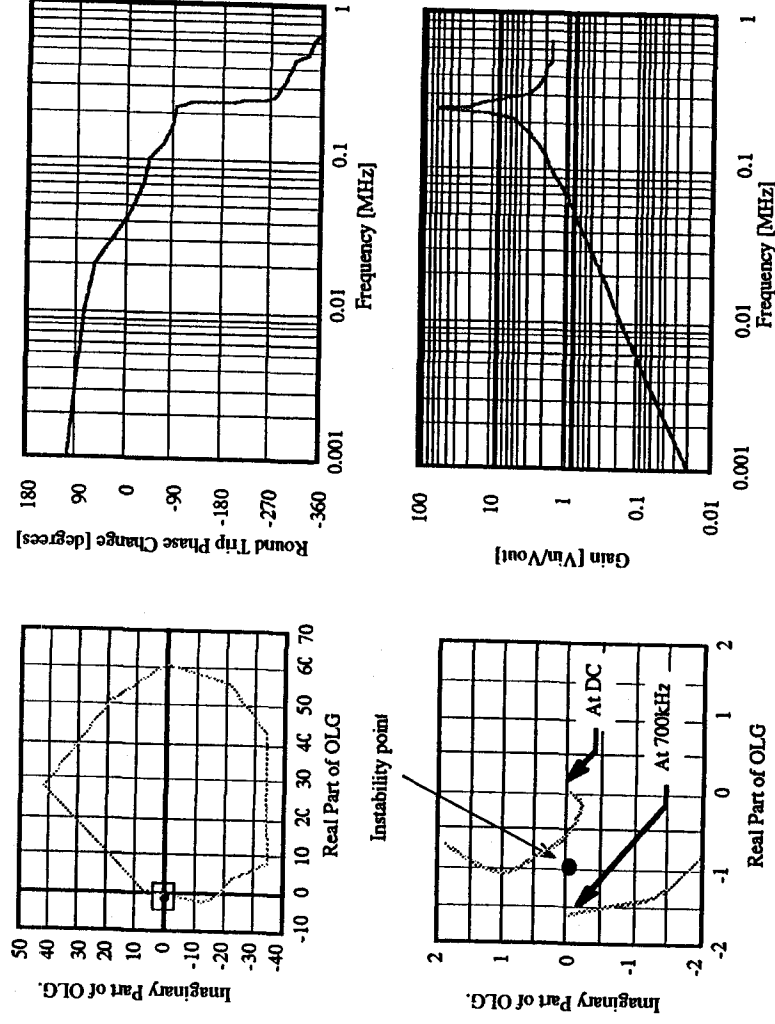


Figure 9b. Open loop characteristics of the system when using the feedback loop of fig. 9a. The two graphs on the left are Nyquist diagrams of the open loop gain (OLG), the bottom left is an expansion in the region of the instability point (-1,0). The graph on the top left shows that the controller has high open loop gain in the positive real section of the Nyquist plane and hence large suppression of noise is possible. The graph on the bottom left shows region centered at (-1,0) which implies that an increase of noise is expected (and present as shown in fig. 10). However, the measured data in the region of the instability point suffers from a low signal to noise ratio due to excessive stray noise near unity gain. The loop was not unstable, as maybe inferred from the diagram. The graphs on the right are Bode plots of the same information. Top right shows the open loop phase change, and the bottom left shows the open loop gain as functions of frequency.

The Nyquist and Bode¹⁵ diagrams of the open loop gain (OLG) in this loop are shown in figure 9b. The Nyquist diagrams (left top and bottom) show that the gain of this system is high for most of the loop and hence a large reduction in the relaxation oscillation is possible, but the loop enters the region enclosed by a circle of unity length centred at the instability point (-1,0). Consequently, an increase in noise at some frequency is inevitable. The Bode diagrams (right top and bottom) show the loop gain and round trip phase as a function of frequency. Around the frequencies 60 kHz and 700 kHz the gain is greater than 1 and simultaneously the phase is approaching positive feedback. At these frequencies the noise is increased.

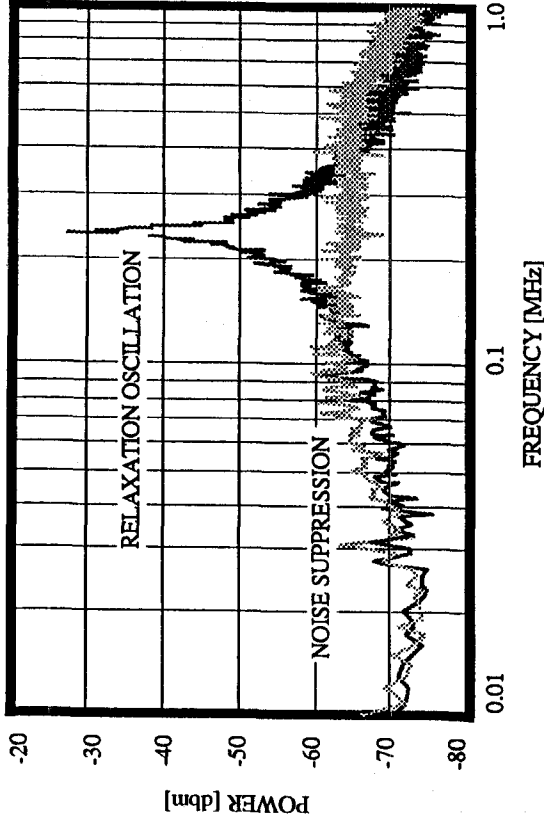


Figure 10a. Noise suppression produced using control loop 2. The noise was reduced at the rel. osc. frequency by 40 dB, however the noise increased by 2-3dB at frequencies close to the rel. osc. Hence only 35dB noise suppression is produced over all. The noise increased in those regions indicated by the Nyquist plots of figure 9.

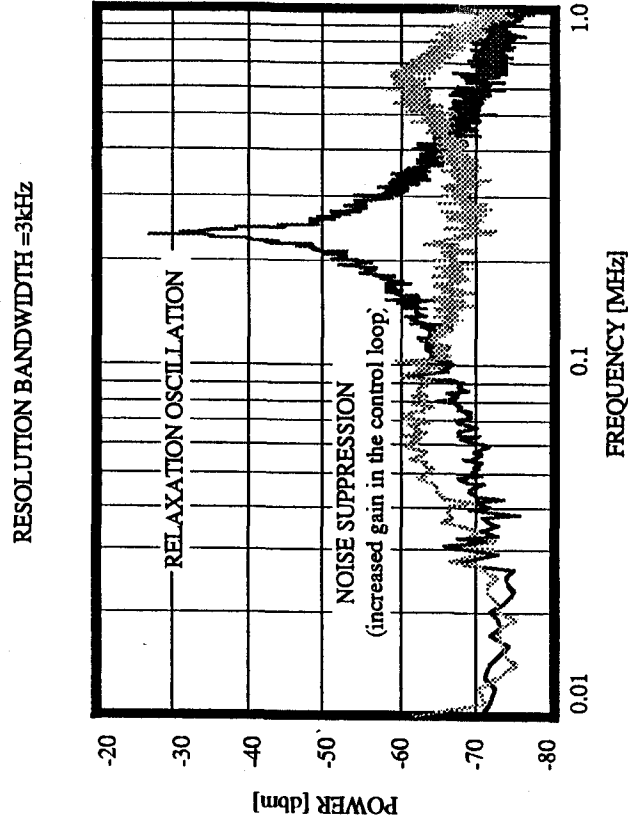


Figure 10b. Noise suppression produced using control loop 2, but deliberately increasing the loop gain in comparison to fig. 10a. This scan shows that the noise at the rel. osc. frequency can be reduced by at least 50dB using this control loop. A consequence is that the noise is increased at other frequencies, however with better control electronics the increased noise could be eliminated.

The noise suppression achieved by this loop is shown in figure 10. We show two noise traces to illustrate the effect of increasing the gain in the control loop. Figure 10a has the gain characteristics shown in figure 9b, while 10b has (intentionally) greater overall loop gain. We

could obtain 40dB of noise reduction at the relaxation oscillation frequency when using the gain setting of 10a. Increasing the loop gain resulted in a suppression of 50dB, but the noise in the region of 60 kHz and 700 kHz was increased as well, to the point that the over all suppression was no better than that of 10a. The noise increase near 60kHz increased due to incorrect positioning of the roll over frequency of the differentiator, so with better adjustment it could be eliminated. The noise increase near 700kHz, on the other hand, is due to several factors. Firstly, the all pass filter caused an unacceptable time delay in the loop. Also, the op-amps have phase problems at these frequencies when operating with high gain. So faster op-amps are required for these high frequencies.

One final control loop (3) was tested during this project. It was based on an active integrator circuit, the design is shown in figure 11. Two sections are present here as well. The first is the integrator section which has a roll over frequency of 5.9kHz, followed by a unity gain inverting amplifier which is placed in the circuit to get the correct phase for the feedback signal. In between the two sections is a 470nF capacitor that is used to eliminate any DC components arising from imbalances in the op-amps.

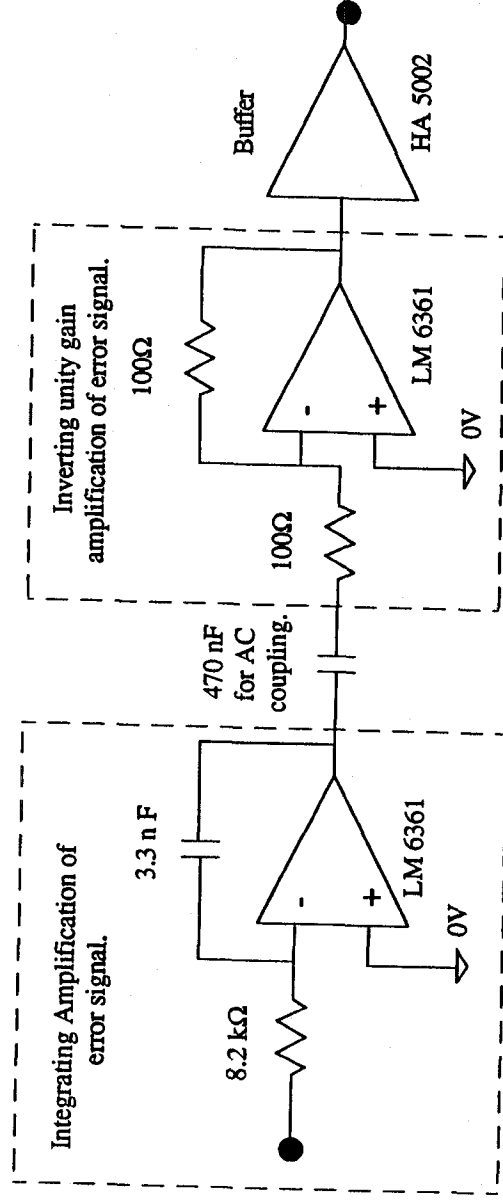


Figure 11. Circuit diagram for control loop 3. The circuit is based on an active integrator, roll over frequency is at 5.9kHz. A 470nF capacitor is placed in the circuit to eliminate some DC signals arising from imbalances in the op-amp in the circuit. It will be removed in the final control loop. An inverting unity gain amplifier is used to produce the correct phase for the feedback signal.

This type of amplifier is generally used to suppress low frequency noise. In this case we were interested to see if we were able to reduce the noise below the relaxation oscillation frequency. The results, figure 12, show that it is possible to reduce the laser noise at low frequencies. We were able to suppress the laser noise below 60kHz, and found that up to a frequency of about 20kHz the noise suppression reached the shot noise limit. Above 60kHz the remaining noise

contains two maxima at two distinct frequencies. These noise maxima arose from incorrect correction signal feedback at these frequencies.

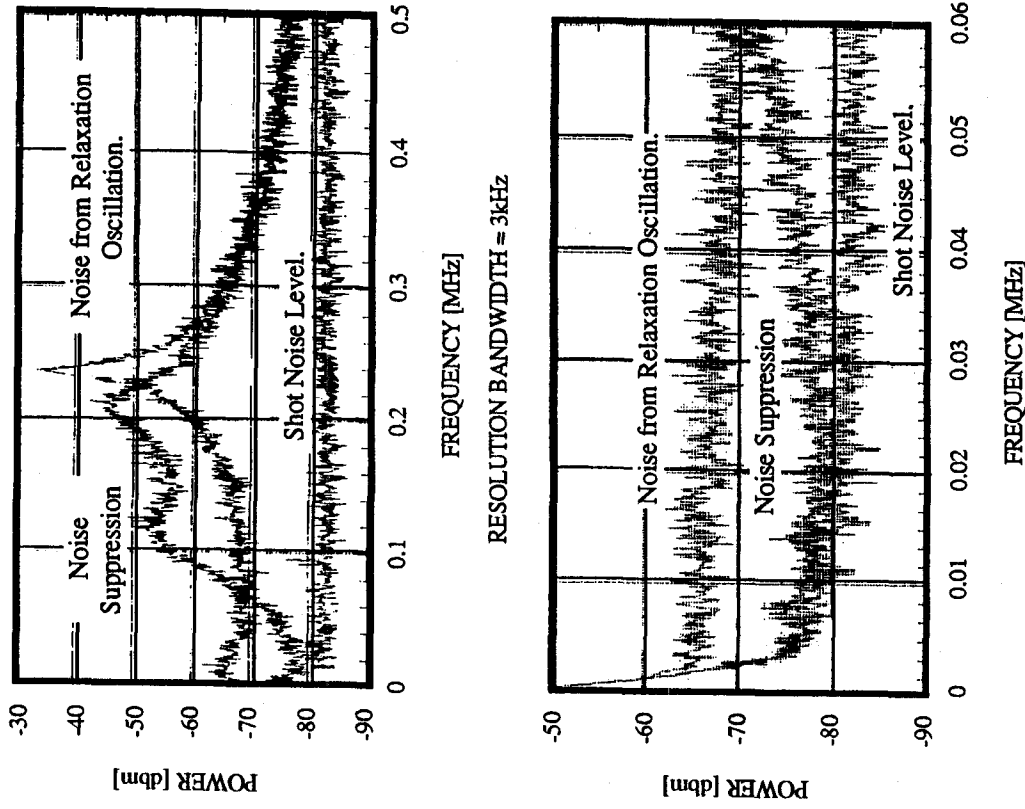


Figure 12. Noise suppression achieved using control loop 3. The top spectrum analyser scan shows the noise from the relaxation oscillation; the noise suppression achieved from control loop 3; and the shot noise limit for the intensity of white light falling on the monitoring photo-detector. This scan shows the total effect of the control loop on the noise spectrum of the laser, over a frequency range DC to 500kHz (the rel. osc. frequency is at 240kHz). The lower spectrum analyser scan shows the same information over a frequency range from DC to 60kHz. We observe that the rel. osc. noise is suppressed to the shot noise level up to 20kHz by this control loop.

Recommendations for Future Developments

No attempts were made at that stage to combine the three types of control loops because of time and equipment restrictions on the project. We have, however, enough information to design a controller that could reduce the RIN to the shot noise limit. This design is shown in figure 13. This controller is a cascaded PID amplifier. The first stage has the properties of an integrator working with restricted gain at low frequencies. It is followed by a section that has the properties of a differentiator that has restricted high frequency gain. The integrator section controls the low frequency noise (DC to 100kHz), the differentiator section controls the high frequency noise (200 kHz -2MHz), and in the intersecting frequency region both control the intensity noise.

The Gain versus frequency curve shown in figure 13 illustrates the frequency response of the total control loop. The solid curve shows the response of the total controller (including the laser) in comparison to the relaxation oscillation (dashed curve). The roll over frequencies will be determined experimentally.

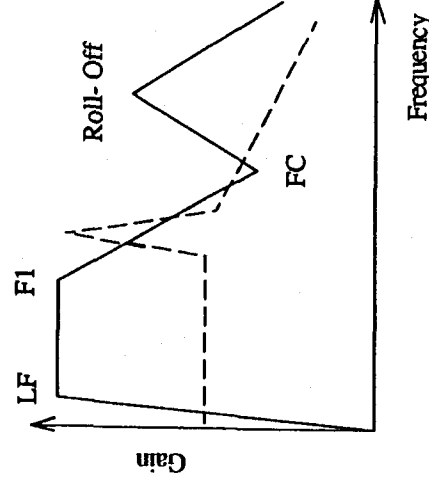
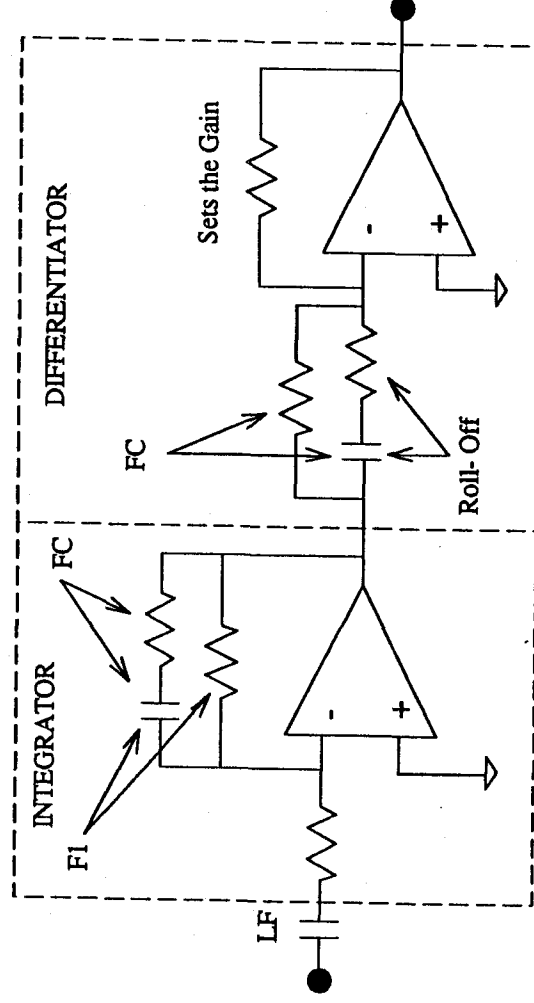


Figure 13. Proposed circuit design for final control loop. This has an active integrator followed by an active differentiator. The corner frequencies for all the different sections are shown in the diagram. Their exact positions are set by the components indicated, and will be tailored experimentally to give the best result.

Conclusion

This collaboration successfully determined the techniques required to control the intensity noise on the output of a diode pumped Nd:YAG non-planar monolithic ring oscillator. We were able to design and test control loops that achieved independently one of the three following results: reduced the amplitude of the relaxation oscillation by a factor of 40-50dB; reduced the noise at frequencies above the relaxation oscillation by several dB; and reduce the low frequency noise (<20kHz) to the shot noise limit. Thus it has been demonstrated that the LZH laser system is suited for the quantum noise limited measurements. Future research should be directed towards the design of an integrated PID controller achieving these results simultaneously. At the same time it has to be investigated whether this feedback control system has any undesirable effects on the frequency noise spectrum, as it has been predicted by other research groups^{1,6}.

Acknowledgments

The authors of this report would like to thank firstly DITAC for funding this collaboration, and the scientists at the Max Planck Institut für Quantenoptik, Garching, Germany, namely Dr. Schilling, Dr. Strain and Prof. Danzmann and also the scientists at the University of Glasgow, Scotland namely Dr. Campbell, Ms. Rowan, and Prof. Hough for their assistance and helpful suggestions during the course of this work.